Brain Structure and Function (2020) 225:45–56
https://doi.org/10.1007/s00429-019-01983-w

ORIGINAL ARTICLE

Perineuronal net expression in the brain of a hibernating mammal

Anna Marchand[1] · **Christine Schwartz**[1]

Received: 25 April 2019 / Accepted: 9 November 2019 / Published online: 21 November 2019

Abstract

During hibernation, mammals like the 13-lined ground squirrel cycle between physiological extremes. Most of the hibernation season is spent in bouts of torpor, where body temperature, heart rate, and cerebral blood flow are all very low. However, the ground squirrels periodically enter into interbout arousals (IBAs), where physiological parameters return to non-hibernating levels. During torpor, neurons in many brain regions shrink and become electrically quiescent, but reconnect and regain activity during IBA. Previous work showed evidence of extracellular matrix (ECM) changes occurring in the hypothalamus during hibernation that could be associated with this plasticity. Here, we examined expression of a specialized ECM structure, the perineuronal net (PNN), in the forebrain of ground squirrels in torpor, IBA, and summer (non-hibernating). PNNs are known to restrict plasticity, and could be important for retaining essential connections in the brain during hibernation. We found PNNs in three regions of the hypothalamus: ventrolateral hypothalamus, paraventricular nucleus (PVN), and anterior hypothalamic area. We also found PNNs throughout the cerebral cortex, amygdala, and lateral septum. The total area covered by PNNs within the PVN was significantly higher during IBA compared to non-hibernating and torpor ($P < 0.01$). Additionally, the amount of PNN coverage area per Nissl-stained neuron in the PVN was significantly higher in hibernation compared to non-hibernating ($P < 0.05$). No other significant differences were found across seasons. The PVN is involved in food intake and homeostasis, and PNNs found here could be essential for retaining vital life functions during hibernation.

Keywords Hibernation · Perineuronal nets · Paraventricular nucleus · Torpor

Introduction

Mammalian hibernation is an adaptation that allows some mammals, like the 13-lined ground squirrel (*Ictidomys tridecemlineatus*), to survive periods of time in extreme and harsh environments with few resources. Hibernation provides a unique opportunity to study plasticity and neuroprotection in the brain, because the ground squirrel brain undergoes extensive alterations that accompany extreme changes in whole body physiology (Fig. 1). Throughout hibernation, the ground squirrels cycle between lengthy torpor bouts (7–10 days) and brief interbout arousals (IBAs, 12–24 h) (Carey et al. 2003). During torpor, in addition to near-freezing body temperatures, 13-lined ground squirrels also have a depressed heart rate and reduced blood flow to the brain (Frerichs et al. 1994, Carey et al. 2003). However, the ground squirrels rapidly return to non-hibernating physiological conditions during IBA. These changes in physiology repeat throughout the hibernation season. During torpor, some areas of the forebrain, including the cerebral cortex and hippocampus, exhibit synaptic disorganization and regression of dendritic spines, which is associated with low body temperature (Popov et al. 1992, Magariños et al. 2006, von der Ohe et al. 2006, 2007). Connected neurons normally form a functional network for transfer of information; so, alteration of synapses in torpor presumably removes or alters the ability of these neurons to communicate. Supporting this, electroencephalogram (EEG) data from the cerebral cortex during torpor indicate that this area of the brain is electrically quiescent (Heller 1979). The neurons must reconnect and regain activity sometime during the return to IBA, as the synapses are reorganized during this brief time. This neuronal plasticity is thought to be widespread through the brain, but so far no investigation of synapse organization or

Electronic supplementary material The online version of this article (https://doi.org/10.1007/s00429-019-01983-w) contains supplementary material, which is available to authorized users.

✉ Christine Schwartz
cschwartz@uwlax.edu

[1] Department of Biology, University of Wisconsin-La Crosse, 1725 State St., La Crosse, WI 54601, USA

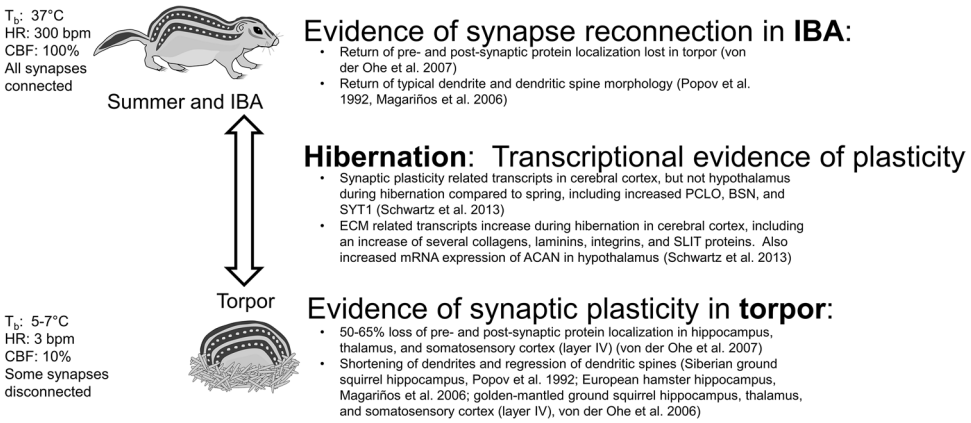

Fig. 1 Summary of 13-lined ground squirrel seasonal physiological changes. Torpor and IBA are the two extremes of hibernation and the animals cycle between these states throughout hibernation. Torpid animals exhibit physiological depression and undergo changes within the brain, specifically a disconnection of some synapses. By the time the animal reaches IBA, the brain and physiological parameters return to states seen in the typical non-hibernating ground squirrel. Ground squirrels in IBA exhibit similar physiological phenotypes to animals in summer. In addition to information about synapse state provided for torpor and IBA, transcriptional evidence of plasticity and remodeling observed during hibernation compared to spring, non-hibernating animals is provided. This figure was based on data from several sources in addition to those provided (Frerichs et al. 1994, Carey et al. 2003, von der Ohe et al. 2007). *CBF* cerebral blood flow, *HR* heart rate, *IBA* interbout arousal, T_b body temperature

plasticity has focused on areas of the brain like the hypothalamus or brain stem that might need to retain some function during hibernation, or at least during early arousal, before the brain has fully warmed. EEG recordings indicate that the hypothalamus and parts of the brain stem maintain some activity even during torpor (Heller 1979).

Transcriptomic evidence from the 13-lined ground squirrel hypothalamus indicates that the extracellular matrix could be important in promoting function during hibernation. This work showed that mRNA expression of aggrecan (*ACAN*), an important component of perineuronal nets (PNNs), is significantly increased during hibernation and the fall transition before hibernation in the hypothalamus (Schwartz et al. 2013, 2015). PNNs are specialized extracellular matrix structures known to restrict the plasticity of neurons. The sheath-like nets cover the outside of neurons, stabilizing existing connections and preventing new ones (Wang and Fawcett 2012). They are also known to be protective to neurons. Previous work investigating the pathology of Alzheimer's disease in post-mortem human brains showed that neurons covered with PNNs were protected from neurodegeneration (Brückner et al. 1999, Morawski et al. 2010). This net-specific protection was also shown in a cell culture model of Alzheimer's disease, which additionally reported that removal of the nets from neurons eliminated the protection (Miyata et al. 2007). PNNs are also protective against oxidative stress (Cabungcal et al. 2013). These studies indicate that PNNs are protecting the wrapped neurons and that the neurons without the protective nets are more susceptible to damage and death, which ultimately can result in functional losses. Seasonal formation or alteration of PNNs could be very important in the 13-lined ground squirrel brain for retaining hypothalamic function during hibernation and preparation for hibernation, by potentially both protecting neurons from damage and preventing temperature-dependent synaptic plasticity to retain function. Here, we investigate seasonal expression of PNNs in the 13-lined ground squirrel forebrain, focusing specifically on the hypothalamus.

Methods

Animals

Both captive bred and wild-caught 13-lined ground squirrels (*Ictidomys tridecemlineatus*) were used in these experiments. The wild caught animals were captured in accordance with a Scientific Collectors permit from the Wisconsin Department of Natural Resources in the spring in La Crosse County, WI on private property with permission. All ground squirrels were housed upon arrival in the Association for Assessment and Accreditation of Laboratory Animal Care International (AAALAC-I) accredited Animal Care Facility located at the University of Wisconsin-La Crosse. Captive bred animals were born in this facility. Animals were housed individually in standard plastic guinea pig cages (13 × 17 × 8 inches) with wire tops containing aspen bedding. All animals were provided a tunnel and nesting material (Enviro-Dry) as environmental enrichment. During the non-hibernating season, the ground squirrels were kept at room temperature (set to 21 °C) with a natural light/dark cycle matching the area. They were provided with Teklad

2018 Rodent Diet and water ad libitum. Teklad Cat Diet and supplemental sunflower seeds were also provided as needed. In fall, the animals were housed in 7″ × 12″ × 5″ mouse cages and provided with extra bedding material before being moved into an environmental chamber for hibernation (constant darkness, 6–8 °C). The ground squirrels were not provided with food or water during their hibernation in the lab. Body temperature of the experimental animals was taken at the time of tissue collection (Table S1). All experimental procedures were approved by the University of Wisconsin-La Crosse Institutional Animal Care and Use Committee (protocol #14–15).

Experimental collection points

Nineteen ground squirrels were used for these experiments, in three collection points: Torpor (7), IBA (6), and Summer (non-hibernating, 6). Both males and females were used, as both sexes exhibit the extreme changes in hibernation physiology in the lab. No differences were found between males and females.

The torpor and IBA collection points provide the two extremes of the hibernation cycle. In torpor, the ground squirrels exhibit near freezing body temperatures, low heart rates, and low oxygen consumption, while all of these physiological parameters return to normothermic levels at IBA (Carey et al. 2003). Animals were checked daily, but in an effort to keep hibernation conditions and transitions between torpor and IBA as natural as possible, the animals were not handled and body temperature was not rectally assessed, as this could affect arousal parameters or trigger a premature arousal. Therefore, the exact timing of killing within the torpor bout and IBA is not known. Torpid state was verified at killing by rectal body temperature (7.29 ± 0.29 °C, Table S1). All animals used for the IBA collection point aroused spontaneously, were observed as awake and active (eyes open and exhibiting coordinated movements), and were torpid the previous day. IBA animals had an average rectal body temperature of 31.5 ± 0.67 °C (Table S1) at the time of killing. The hibernation collection point animals (Torpor and IBA) were killed during January and February when average torpor bout length is the longest. The Summer collection point occurred in early summer (April–May), when the animals were active and not hibernating.

Brain dissection and cryosectioning

All animals were fully anesthetized with Isoflurane and then killed by decapitation. The brain dissection was performed on ice. The brain was removed from the skull and the meninges and blood vessels surrounding the brain were removed. The brain was blocked on both sides, removing cerebellum, brain stem, and prefrontal cortex. The hypothalamus was retained and intact after the blocking. The blocked brain was covered in optimum cutting temperature (OCT) medium, flash frozen in isopentane (2-methylbutane) cooled with dry ice, and stored at -80 °C until use.

Serial coronal sections (18 µm) of each brain were cryosectioned, thaw mounted onto superfrost plus microscope slides, and stored at − 20 °C until use. Serial adjacent brain sections were separated into ten sets of slides. One slide set from each animal was used for *Wisteria floribunda* lectin histochemistry (see below), one set was stained with cresyl violet to help verify brain anatomy, and additional slide sets served as replacements or were used in other experiments.

Fluorescent lectin histochemistry with Nissl stain

Brain sections on each slide were encircled with a hydrophobic barrier (GnomePen, Invignome) and then fixed in 2% paraformaldehyde in Tris buffered saline (TBS). Then, the sections were blocked in blocking solution (1% bovine serum albumin in TBS-Triton (TBS-TX; TBS with 0.05% Triton-X 100)), and incubated in biotinylated *Wisteria floribunda* lectin (1:165; Sigma-Aldrich, #L1516) in blocking solution for 2 h. The sections were then held overnight in TBS-TX at 4 °C. The next day, the sections were incubated in streptavidin with an Alexa Fluor® 488 Conjugate (1:100; Thermo-Fisher, #S32354) in TBS-TX for 1 h. Finally, the sections were incubated in NeuroTrace™ 530/615 Red Fluorescent Nissl Stain (1:250; Thermo-Fisher, #N21482) in TBS for 30 min. The slides were coverslipped using Fluoromount and stored at 4 °C. All steps were completed at room temperature unless stated otherwise. For a control, the lectin histochemistry protocol was also performed in the same manner without *Wisteria* lectin during the 2 h incubation, which resulted in no staining (Fig. S2). *Wisteria* lectin is known to be a reliable stain for PNNs, shown through many studies combining lectin histochemistry with immunohistochemistry for aggrecan and other PNN components (Dityatev et al. 2007; Giamanco et al. 2010, Morawski et al. 2014). Previous work showed that *Wisteria* lectin staining is specific to chondroitin sulfate epitope of aggrecan (Giamanco et al. 2010). It must be noted that this method does have limitations, and would be bolstered by the use of other markers of PNNs which can reveal some of the microstructure of individual PNNs (Matthews et al. 2002). However, commercially available monoclonal antibodies were not compatible with our study species; so, we were not able to include this further validation.

Imaging and data analysis

The hypothalamus was the primary focus of this work, based on previous transcriptome data, and preliminary work identified three hypothalamic nuclei that exhibited consistent

staining and thus were selected for analysis. These regions of interest (ROIs) were the ventrolateral hypothalamus (VLH), anterior hypothalamic area (AHA), and paraventricular nucleus (PVN). The VLH identified in this study was anterior to the AHA and PVN, lateral to the third ventricle, and superior to the optic chiasm. Based on the anatomy, the VLH is most likely the ventrolateral portion of the medial preoptic area, but the ventrolateral preoptic area is directly adjacent to this nucleus; so, as mentioned in previous studies (Bratincsak et al. 2007), it is difficult to confidently differentiate between them. The PVN is an anatomically obvious nucleus with tightly packed neurons spanning the third ventricle. The AHA is lateral and inferior to the PVN.

While specific nuclei of the hypothalamus were the ROIs for this experiment, preliminary work also highlighted several other ROIs to include in the analysis: cerebral cortex, lateral septum, and amygdala. These regions are quite large and PNN staining was found throughout each region, so analysis was focused on specific areas of these ROIs according to the neuroanatomy, to be consistent across individuals. Analysis of the cerebral cortex focused on cingulate cortex and two areas of sensorimotor cortex, dorsal and dorsolateral cortex. Analysis of these three cerebral cortex areas occurred just anterior to the first sighting of the CA3 area of the hippocampus. Analysis of the lateral septum was focused on dorsal lateral septum just anterior to where the fornix and anterior commissure meet centrally. Analysis of the amygdala was focused on the same brain sections where the PVN of the hypothalamus was located. All analyzed sections of amygdala exhibited a distinct crescent shape, as seen in the rat brain described as anterior amygdaloid area (Paxinos and Watson 2005). All anatomical distinctions were made using a rat brain atlas, along with reference to a ground squirrel atlas with considerably less detail (Joseph et al. 1966, Paxinos and Watson 2005). All analyzed regions are illustrated in Fig. 2. These atlas images were drawn in our lab using cresyl violet stained sections from a representative brain.

Images of each brain region were taken with a digital camera on a Nikon Eclipse Ni fluorescence microscope and then analyzed in ImageJ. Each image was thresholded to highlight cells from background staining (using the auto threshold function) and converted to a binary image for analysis; so all pixels of the cells that were above background were black and the background was white. This included all parts of the cells, specifically including both cell bodies and any wrapped dendrites. Examples from cingulate cortex and PVN are provided in Fig. S1. This method of thresholding was used to be as consistent as possible across images (Arena et al. 2017). Particle size was restricted to 250–4000 pixels for the cell counts, to focus specifically on whole cells. Number of PNN covered cells and total PNN coverage area were measured for each region in this analysis. Total PNN coverage area compiled all the black pixels in the selected analysis area of the binary image to compare PNN coverage area between seasons in addition to total number of PNN covered cells. In addition to total PNN coverage area, % area was also compiled and analyzed, which reflects percentage of PNN coverage in the analysis area. Additionally, mean staining intensity was analyzed for all brain regions, to investigate any differences across groups for each brain region.

Analysis parameters varied by brain region, due to differences in overall size and staining. In the dorsal and dorsolateral cerebral cortex, staining was analyzed in layers III and

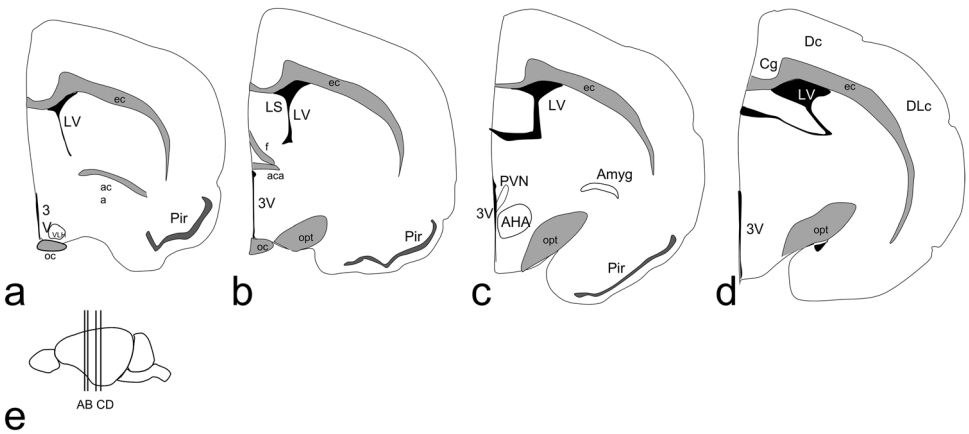

Fig. 2 Atlas drawings of 13-lined ground squirrel brain. **a**–**d** provide specific anatomical landmarks and areas of analysis for the brain regions examined in this manuscript. A sagittal view of the ground squirrel brain is provided in e, indicating the location of the brain slices shown in **a**–**d**. This atlas was drawn in our lab from images of a representative cresyl violet stained brain. *3V* third ventricle, *aca* anterior commissure, *AHA* anterior hypothalamic area, *Amyg* amygdala, *Cg* cingulate cortex, *Dc* dorsal cerebral cortex, *DLc* dorsolateral cerebral cortex, *ec* external capsule, *f* fornix, *LS* lateral septum, *LV* lateral ventricle, *oc* optic chiasm, *opt* optic tract, *Pir* piriform cortex, *PVN* paraventricular nucleus, *VLH* ventrolateral hypothalamus

V, where nets were concentrated, using a 175.8 × 175.8 μm^2 box. The same analysis parameters were used in the anterior cingulate cortex, but the box was focused in the center of the structure. A 58.6 × 58.6 μm^2 box was used for amygdala and lateral septum to fit the bounds of the structures better than the larger box used in the cortex regions. Five consecutive sections were measured for the cerebral cortex regions and lateral septum and three for the amygdala, according to the neuroanatomy as discussed in the previous paragraph. In the hypothalamus, the smaller size of the nuclei (PVN, AHA, VLH) allowed for analysis of the full structure. A polygon was created in ImageJ to surround the specific PNN-stained area (a representative example from PVN analysis is provided in Fig. S1). The cells in the PVN and VLH were too intensely stained and the PNN-stained cells were too closely packed together, that it was not possible to count individual PNN-stained cells in this area, so the initial analysis focused on total lectin stained area only. Regardless of the initial size of the analysis area, all PNN-wrapped cell counts and total PNN coverage area for each brain region analyzed were converted into cells/coverage area per 100 μm^2 to facilitate comparison across brain areas.

For PVN, an additional analysis was performed, where Nissl stained neurons were also analyzed in the polygon along with the lectin staining. For Nissl-stained neurons, overall neuron number and total coverage area were analyzed, along with PNN coverage per Nissl-stained cell, and the percentage of Nissl area covered by PNNs. The lectin histochemistry protocol with Nissl staining was repeated twice for the PVN on different adjacent sections from the same animals to verify the results obtained.

Not all animals were used for each brain region analysis due to availability of sections that met the anatomical criteria outlined above. A minimum of four brains were used for each experimental group for each brain region. The means for PNN covered cell count, total stained area, % area, and mean staining intensity were calculated for each brain region in each animal. The means for each brain region were compared across the three experimental groups using an analysis of variance (ANOVA) with post hoc Tukey's range test in SPSS.

Results

PNN-wrapped cells are found across all time points in all brain regions analyzed

Table 1 summarizes the mean number of PNN-wrapped cells per μm^2 in the three areas of cerebral cortex, amygdala, lateral septum, and anterior hypothalamic area across torpor, IBA, and summer (non-hibernating). PNN-wrapped cells appear in all seasons in all brain structures analyzed and no significant differences in cell count were found across the three groups for any of these brain regions. Representative images of PNNs in each of the analyzed brain regions from torpor and IBA animals are shown in Fig. 3.

Importantly, in the cerebral cortex, PNNs were widespread throughout this large brain region, but the analysis presented here focuses on specific cortical regions detailed in the methods. Additionally, the PNNs appear specifically concentrated layers III and V, which is particularly noticeable in dorsal and dorsolateral cortex (Fig. 3a). Cells in both layers were analyzed separately in dorsal and dorsolateral cerebral cortex, but no significant differences between collection groups were found. Interestingly, overlay of Nissl staining with lectin histochemistry reveals that the PNNs do not surround all cells within the cerebral cortex, but wrap a certain population of neurons (Fig. S3). The PNN-wrapped neurons exhibit a basket cell-like anatomy, characteristic of some neurons found in layers III and V (Fig. 4a).

PNNs in the amygdala were not only prominent within the anterior amygdaloid area (Fig. 3b), but also found throughout the amygdala. In the septum, PNNs were found in the lateral septum, extending across the entire structure, but analysis and imaging focused on the most superior portion, corresponding to dorsal lateral septum (Fig. 3c). PNNs were not found in the neighboring medial septum. PNN-wrapped cells in both lateral septum and amygdala showed staining around the cell bodies, but staining of the dendrites did not appear as prominent as in the cerebral cortex.

Within the hypothalamus, cell counts were only analyzed in anterior hypothalamic area (Fig. 3d). Here, some

Table 1 Summary of mean number of PNN-wrapped cells per 100 μm^2 in analyzed brain regions. Analysis areas for each region are detailed in the methods. Data are shown as mean ± standard error of the mean

Brain region	Summer (*n*)	Torpor (*n*)	IBA (*n*)	*P* value	*F* (*d.f.*)
Amygdala	21.71 ± 1.84 (5)	21.28 ± 1.21 (7)	20.00 ± 1.22 (5)	0.71	0.35 (16)
Lateral septum	28.23 ± 2.73 (4)	25.42 ± 0.99 (7)	24.85 ± 2.17 (5)	0.46	0.84 (15)
Cingulate cortex	4.35 ± 0.43 (6)	4.28 ± 0.30 (7)	5.37 ± 0.56 (6)	0.17	1.99 (18)
Dorsal cortex, Layer III	1.67 ± 0.29 (5)	3.25 ± 0.36 (7)	3.47 ± 0.85 (5)	0.07	3.22 (16)
Dorsal cortex, Layer V	3.24 ± 0.24 (5)	3.70 ± 0.30 (7)	4.36 ± 0.67 (5)	0.23	1.63 (16)
Dorsolateral cortex, Layer III	2.69 ± 0.56 (5)	3.60 ± 0.63 (7)	3.84 ± 0.89 (5)	0.52	0.68 (16)
Dorsolateral cortex, Layer V	3.61 ± 0.36 (5)	3.86 ± 0.43 (7)	4.30 ± 0.51 (5)	0.59	0.54 (16)
Anterior hypothalamic area	4.50 ± 0.59 (4)	4.17 ± 0.36 (6)	4.02 ± 0.28 (4)	0.76	0.29 (13)

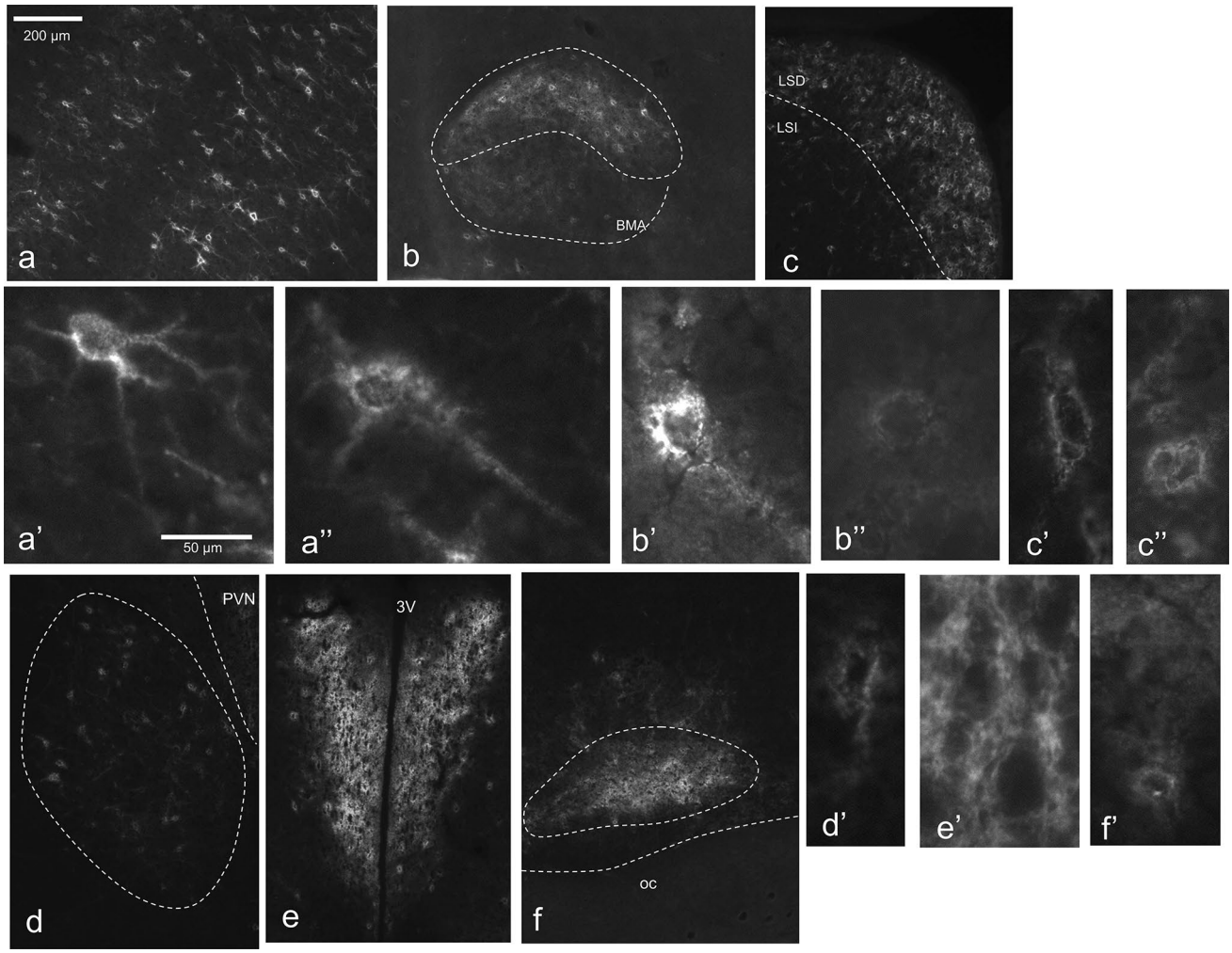

Fig. 3 Localization of perineuronal nets in ground squirrel brain. **a** Dorsolateral cerebral cortex with prominent staining in layers III (**a′**) and V (**a″**). **b** Amygdala with representative cells from AA (**b′**) and BMA (**b″**). c. Lateral septum with representative cells from LSD (**c′**) and LSI (**c″**). **d** and **d′**. Anterior hypothalamic area. **e** and **e′**. Paraventricular nucleus. **f** and **f′**. Ventrolateral hypothalamus. All images were obtained with *Wisteria floribunda* lectin histochemistry and are representative images taken from torpor (**a**, **c**, **e**) and IBA (**b**, **d**, **f**). Summer animals are not shown, but exhibited the same staining patterns. Scale bar in **a** applies to images in **a**–**f**. Scale bar in **a′** applies to all ′and ″ images. *3V* third ventricle, *AA* anterior amygdaloid area, *BMA* basomedial amygaloid nucleus, *III* cerebral cortex layer III, *V* cerebral cortex, layer V, *LSD* dorsal lateral septum, *LSI* intermediate lateral septum, *LV* lateral ventricle, *oc* optic chiasm, *PVN* paraventricular nucleus

of the cells exhibited prominent PNN-wrapped dendrites (Fig. S3). Cell counts were not analyzed in PVN or VLH due to cell density and overlapping of PNN staining, but staining can clearly be seen in all seasons in these areas as well (Fig. 3e, f).

PNNs specifically surround neurons

To confirm that PNNs were covering neurons specifically, lectin histochemistry for PNNs was paired with a fluorescent Nissl stain for neuron cell bodies, which allowed for overlay of the two stains. Figure 4 shows a representative image from anterior cingulate cortex showing that the PNNs cover the cell bodies of neurons, along with extending out along the dendrites. Cells in all other brain regions were also verified as neurons in this manner (Fig. S3).

PNN coverage area is significantly greater during hibernation in the PVN of the hypothalamus

Table 2 summarizes the mean total PNN-stained area per 100 µm^2 and mean percent coverage area in all regions analyzed for comparison across brain regions. In the PVN, total PNN-stained area is higher in IBA compared to both torpor and summer (PNN coverage area (total area of coverage across whole nucleus, µm^2): Summer:

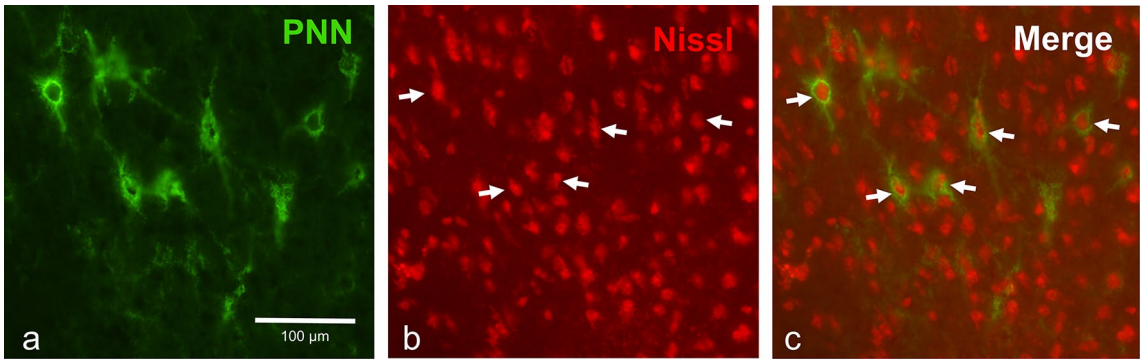

Fig. 4 Perineuronal nets surround neurons. **a** PNN staining via lectin histochemistry in cingulate cortex (green). **b** Nissl staining of cell bodies in cingulate cortex (red). White arrows point to cell bodies clearly surrounded by PNNs shown in c, while many other cell bodies are present but uncovered. **c** Merging of PNN and Nissl staining reveals that PNNs surround neuron cell bodies and extend out onto dendrites. Scale bar applies to all images

Table 2 Summary of mean PNN coverage area per 100 µm^2 and % coverage area in analyzed brain regions

Brain region	Summer (*n*)	Summer % area	Torpor (*n*)	Torpor % area	IBA (*n*)	IBA % area	*P* value	*F* (*d.f.*)
Amygdala	2659.42 ± 70.07 (5)	26.59 ± 0.70	2274.39 ± 87.01 (7)	22.74 ± 0.87	2474.39 ± 331.23 (5)	24.75 ± 3.31	0.34	1.17 (16)
Lateral septum	1602.95 ± 93.22 (4)	16.03 ± 0.93	1362.62 ± 90.19 (7)	13.63 ± 0.90	1441.91 ± 110.06 (5)	14.42 ± 1.10	0.28	1.39 (15)
Cingulate cortex	299.66 ± 36.91 (6)	3.00 ± 0.37	266.80 ± 26.81 (7)	2.67 ± 0.27	388.93 ± 65.34 (6)	3.76 ± 0.61	0.16	2.03 (18)
Dorsal cortex, Layer III	89.44 ± 20.21 (5)	0.89 ± 0.20	174.29 ± 23.09 (7)	1.75 ± 0.23	207.32 ± 64.20 (5)	2.07 ± 0.64	0.13	2.32 (16)
Dorsal cortex, Layer V	199.87 ± 13.32 (5)	2.00 ± 0.13	232.17 ± 26.00 (7)	2.32 ± 0.26	275.09 ± 50.42 (5)	2.75 ± 0.50	0.33	1.21 (16)
Dorsolateral cortex, Layer III	194.14 ± 35.00 (5)	1.81 ± 0.36	205.45 ± 45.52 (7)	2.18 ± 0.47	267.16 ± 74.96 (5)	2.67 ± 0.75	0.77	0.26 (16)
Dorsolateral cortex, Layer V	245.99 ± 24.14 (5)	2.46 ± 0.24	245.35 ± 35.42 (7)	2.45 ± 0.35	292.41 ± 60.05 (5)	2.93 ± 0.60	0.68	0.40 (16)
Anterior hypothalamic area	313.85 ± 45.80 (4)	3.13 ± 0.46	308.49 ± 43.46 (6)	3.08 ± 0.43	338.46 ± 76.88 (4)	3.38 ± 0.77	0.92	0.08 (13)
Ventrolateral preoptic area	1480.08 ± 118.57 (5)	14.80 ± 1.19	1338.79 ± 191.82 (5)	13.39 ± 1.91	1729.44 ± 347.91 (5)	17.29 ± 3.48	0.52	0.68 (14)
Paraventricular nucleus	1701.48 ± 71.00 (4)	17.01 ± 0.71	1898.87 ± 112.46 (5)	18.99 ± 1.12	2197.91 ± 88.05 (5)	21.98 ± 0.88	**0.013***	6.66 (13)

Analysis areas for each region are detailed in the methods. Data are shown as mean ± standard error of the mean

7231.64 ± 603.01(n = 4); Torpor: 9062.20 ± 601.05(n = 5); IBA: 11752.52 ± 666.12(n = 5); P = 0.001; Fig. 5a). Mean percent coverage area is significantly higher in IBA compared to summer, but neither is significantly different from torpor (P = 0.013, Fig. 5b). Representative images of the PVN are provided in Fig. 5 from animals in summer (c), torpor (d) and IBA (e). No significant differences in total PNN coverage area were found between collection points in any other brain region analyzed, including the other nuclei of the hypothalamus.

Analysis of total PNN-wrapped cells was not possible in PVN because of the density of the cells present there. Since a significant difference in total PNN coverage area and percent coverage area was found in this region, the total number of neurons was also determined, using fluorescent Nissl staining coupled with the lectin histochemistry to stain PNNs. Nissl staining in PVN revealed that total neuron number was significantly lower in torpor compared to IBA, but neither showed a significant difference from summer (Mean neuron count in PVN: Summer: 334.75 ± 8.60 (n = 4); Torpor: 296.27 ± 25.81 (n = 5); IBA: 383.31 ± 8.19 (n = 5); P = 0.012; Fig. 6a). This same pattern is observed in the total area covered by Nissl staining in PVN (P = 0.017; Fig. 6b). Taking the cell number into account for each animal revealed that the PNN coverage per Nissl-stained neuron in the PVN was significantly higher during hibernation (torpor and IBA)

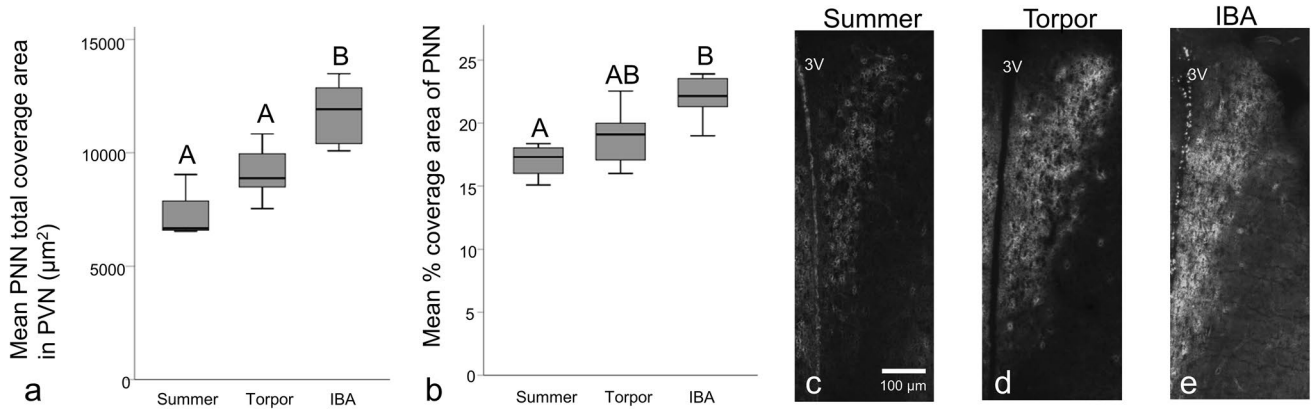

Fig. 5 PNN coverage area and % area in paraventricular nucleus. **a** Quantification of total area covered by PNNs in the PVN in summer, torpor, and IBA, showing that IBA has significantly higher PNN coverage than torpor and summer (ANOVA with Tukey's post hoc test, $P=0.001$). **b** % coverage area of PNN, showing that IBA has a significantly higher % area than summer (ANOVA with Tukey's post hoc test, $P=0.013$). The box plots show the interquartile range of the data, with the edges of the box indicating the first and third quartiles. The centerline of each box indicates the median. The whiskers indicate the maximum and minimum values. Boxes with the same letter are not significantly different from each other. Representative images of PNNs stained with WFA in PVN are shown in **c** (summer), **d** (torpor), and **e** (IBA). Scale bar applies to all images

compared to summer (PNN coverage/cell (µm^2/cell): Summer: 21.61 ± 1.34 ($n=4$); Torpor: 32.84 ± 3.03 ($n=5$); IBA: 30.78 ± 1.38 ($n=5$); $P=0.011$; Fig. 6c). Finally, we investigated the percentage of the Nissl area that was covered by PNN, finding that torpor had significantly higher PNN coverage of Nissl area compared to summer, but neither showed a significant difference from IBA (Summer: 117.98 ± 6.46, Torpor: 201.53 ± 22.47, IBA: 178.57 ± 12.19; $P=0.013$; Fig. 6d). All collection points exhibited over 100% coverage, indicating that PNN coverage extended further than the cell body of the PVN neurons in all cases.

Discussion

This work examined distribution of PNNs in the 13-lined ground squirrel brain, in addition to examining seasonal changes in PNN size and coverage. PNNs were found throughout the cerebral cortex, lateral septum, amygdala, and within some nuclei of the hypothalamus in all time points analyzed. There was a significant seasonal difference in the total area covered by PNNs in the PVN of the hypothalamus, but no other significant differences were found.

PNNs and plasticity during hibernation

PNNs are associated with the end of periods of plasticity. In particular, PNNs are found in the visual cortex after a critical period during juvenile development where incoming sensory input promotes plasticity to achieve appropriate ocular dominance (Pizzorusso et al. 2002). The nets in the visual cortex, and in other areas of the cerebral cortex, mostly surround inhibitory neurons. Once this particular subset of neurons becomes wrapped, they are thought to be stabilized by the PNN, which affects the excitatory and inhibitory balance and ability of the whole circuit to undergo any plasticity (Sorg et al. 2016). As shown in several species, if PNNs are eliminated in the visual cortex, plasticity can occur there again (Carulli et al. 2010, Lensjø et al. 2017). Similarly, PNNs are formed after the critical period in song control nuclei in songbird species, like zebra finches, that learn a song which then crystallizes and cannot be altered once the critical period is over (Balmer et al. 2009).

In the ground squirrel brain, plasticity is characteristic in many neurons as the animal cycles between torpor and IBA. In particular, modifications to microstructural aspects of neurons have been reported in several hibernating species in different brain regions, including cerebral cortex and hippocampus, where dendritic arbors and associated spines retract during torpor, but regrow during active periods (Popov et al. 1992, Magariños et al. 2006, von der Ohe et al. 2006). This suggests that a general disconnection or reduction in connection is occurring during torpor that returns during IBA, supporting the electroencephalography data indicating that many areas of the brain are quiescent during torpor (Heller 1979). Immunohistochemical investigation of synapses, using overlap of pre- and post-synaptic proteins as representative of a synapse, showed that there were less synapses during torpor compared to IBA (von der Ohe et al. 2007). This suggests a disconnection or disorganization of synapses occurring in torpor that reconnect by the time the animal reaches IBA. Additionally, analysis of synapses via electron microscopy reveals changes in the organization of

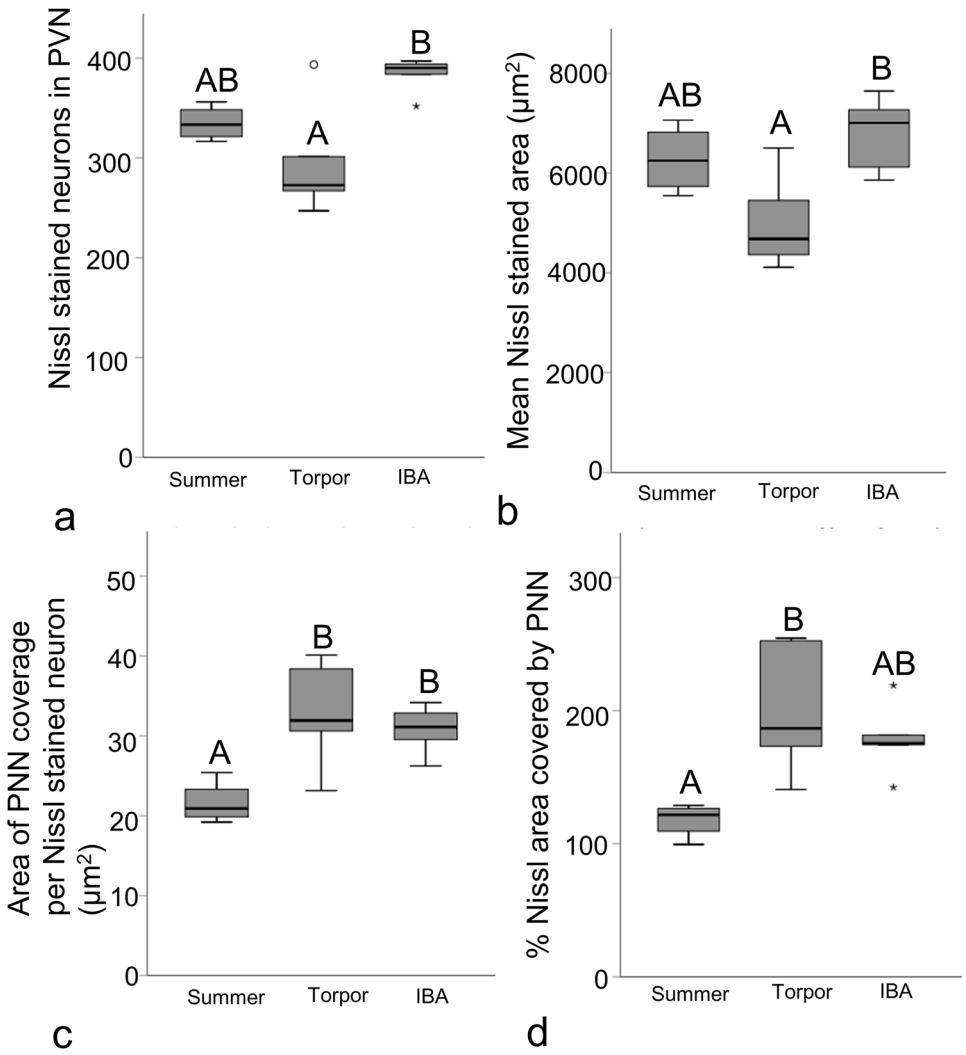

Fig. 6 PNN coverage per neuron in paraventricular nucleus is significantly elevated in hibernation. **a** Quantification of Nissl staining in PVN shows that the number of neurons is significantly lower in torpor compared to IBA, but neither are significantly different from summer (ANOVA with Tukey's post hoc test, $P=0.012$). **b** Analysis of the area covered by Nissl staining shows that Nissl coverage area in IBA is significantly higher than torpor, but neither are significantly different from summer (ANOVA with Tukey's post hoc test, $P=0.017$). **c** Analysis of total PNN coverage area per Nissl-stained neuron in PVN reveals that torpor and IBA have significantly higher coverage than summer (ANOVA with Tukey's post hoc test, $P=0.011$). **d** Analysis of the percent of Nissl area covered by PNNs shows that summer is significantly lower than torpor, but neither are significantly different from IBA (ANOVA with Tukey's post hoc test, $P=0.013$). Boxes with the same letter are not significantly different from each other. The box plots show the interquartile range of the data, with the edges of the box indicating the first and third quartiles. The centerline of each box indicates the median. The whiskers indicate the maximum and minimum values. The open circle and asterisks indicate outliers

synapse structure in cerebral cortex during torpor, although they did not report any synapse loss (Ruediger et al. 2007).

In terms of comparison to other species, the hibernating ground squirrel does not have a critical period per se, but does have a seasonal period where plasticity repeatedly occurs. The presence of perineuronal nets on some neurons and within some brain areas but not others might reflect particular neurons that need to remain connected, and thus are wrapped as a way to restrict the plasticity that occurs in torpor. PNNs are also known to be protective (Brückner et al. 1999, Miyata et al. 2007, Morawski et al. 2010, Cabungcal et al. 2013); so, PNNs could also be important in the hibernator brain to protect particular and important subsets of neurons during a time of extreme physiological transitions in the brain.

PNN coverage increased in the PVN during hibernation

The focus of this work was the hypothalamus, because of preliminary transcriptomic data showing an increase in

aggrecan mRNA during hibernation and the transition to hibernation (Schwartz et al. 2013, 2015). While this lectin histochemistry work did not investigate aggrecan expression directly, it is a reliable marker of aggrecan-based perineuronal nets (Dityatev et al. 2007, Giamanco et al. 2010, Morawski et al. 2014). While nets were found in many brain areas, the only seasonal change in PNNs across seasons was in the paraventricular nucleus of the hypothalamus. Our findings here support previous transcriptome work in the hypothalamus and highlight the PVN as a potentially important brain area for hibernation. Hibernation is characterized by extreme changes in homeostasis, and importantly, while some areas of the body effectively shut down during torpor, some other aspects of physiology remain functional, albeit at depressed levels, including cardiovascular function (Carey et al. 2003). PNNs surrounding neurons in the PVN could provide structural support or protection to facilitate the changes in homeostasis seen during hibernation. The PVN sends many projections to the brain stem, including areas involved in blood flow regulation, gastrointestinal function, and blood pressure regulation, thus playing an important regulatory role in homeostasis (Geerling et al. 2010). Importantly, the PVN sends many projections to the nucleus of the solitary tract, where recent work showed that activation of A1 adenosine receptors in this region induced hypothermia in a non-hibernating species (Tupone et al. 2013). Central activation of the A1 receptor was shown to play a role permitting hypothermia in a hibernating species as well (Jinka et al. 2011). Further, ablation of the PVN in Siberian hamsters disrupted daily torpor (Ruby 1995), again suggesting a vital role for this brain region in the regulation of hibernation and other seasonal phenotypes.

Aside from body temperature and other homeostatic regulation, the PVN could also play an important role in regulation of food intake and monitoring of body adipose stores. 13-lined ground squirrels increase their white adipose tissue in the summer leading up to the hibernation season and then exhibit a drop in food consumption during the fall transition to hibernation, followed by a complete fast during hibernation in the lab (Schwartz et al. 2015). Aggrecan mRNA levels in the hypothalamus increase after this transition in feeding behavior and remain high during hibernation. Previous work indicates that the PVN could function as a kind of adipostat, because it detects both food intake promoting and satiety signals and regulates both energy expenditure and feeding (Cowley et al. 1999). The ability of the PVN to monitor white adipose tissue levels and exhibit control over feeding behavior makes it a likely candidate to be an important driver and regulator of the hibernation phenotype, both during hibernation and in the preparation before hibernation.

Additionally, while the total PNN coverage in the PVN increases during hibernation without taking the number of cells into account, we also found a significant difference in the overall Nissl-stained cell number among the collection points, with fewer cells in torpor compared to IBA. While this was not the focus of the work, this is an interesting finding that is supported by some previous studies. In Arctic ground squirrels, recent work indicated an increased number of thyrotropin releasing hormone (TRH) positive neurons in the PVN of animals in the winter (hibernating) compared to summer (Frare et al. 2019). The authors speculate that this could serve a role in increasing thermogenic capacity during hibernation, but that further studies are needed. Another study investigating frog hibernation, found that cell proliferation increased in the brain during hibernation compared to the active period, which they propose to be a neuroprotective strategy (Cerri et al. 2009). While frog hibernation is distinctly different from mammalian hibernation, both undergo extreme physiological changes. This difference in cell number could also be related to changes in the Nissl substance of the neurons during torpor, although there is no evidence of that in the literature. This increased number of cells during IBA could suggest neurogenesis, and warrants further study, but that is out of the scope of this work.

PNNs in other brain regions

There were no significant seasonal differences in PNNs in other brain regions aside from the PVN of the hypothalamus, but the nets could still be important in these brain regions for hibernation and form sometime between birth and the first onset of torpor. The AHA and VLH of the hypothalamus also contained PNNs. The VLH determined here is in a similar location to the ventrolateral part of the medial preoptic area, which exhibited c-fos expression during entrance to torpor (Bratincsak et al. 2007). The preoptic area and anterior hypothalamus play a role in thermoregulation, specifically in inhibition of heat production (Ishiwata et al. 2002), making this an important area for hibernation. Importantly, the ventrolateral preoptic nucleus, which is involved in sleep regulation (Lu et al. 2000), is also very close to the VLH reported here.

Interestingly, PNNs were found extensively in the cerebral cortex, where aggrecan was very low and not significantly increased during hibernation (Schwartz et al. 2013). In particular, the neurons surrounded by PNNs in the ground squirrel cerebral cortex appear to be the same type of inhibitory neurons wrapped by nets in other species by looking at the basket cell type anatomy (Dityatev et al. 2007), although further work is needed to confirm this. These neurons in other species are thought to be important for excitatory and inhibitory balance in cortical circuits (Sorg et al. 2016), which could be essential for regulating neuron reconnection during IBA in the hibernator brain.

PNNs were also found in the amygdala, which is involved in memory, particularly in relation to emotional or stress related

memory (Roozendaal et al. 2009). Several studies have looked at memory retention in hibernating species over the hibernation season, finding that some types of memory are lost during hibernation while others are retained. In particular, memory related to sociality and recognition of conspecifics is retained (Millesi et al. 2001); so, it is possible that PNNs in amygdala could be important for this type of memory retention from season to season.

Finally, PNNs were also found in the lateral septum, as previous work indicated could be important for body temperature regulation in hibernation. Specifically, a drop in vasopressin immunoreactivity was shown in this region during hibernation in European hamsters in comparison to summer, non-hibernating animals (Buijs et al. 1986). Additionally, infusion of vasopressin into lateral septum prevented animals from exhibiting drops in body temperature necessary for natural hibernation (Hermes et al. 1993). Again, while no seasonal changes in PNNs were found in any of these brain regions, their locations all indicate that their placement could be important for the first onset of hibernation.

Conclusions

Overall, this work provides a unique look into expression of PNNs, which are modified seasonally in the PVN. Further work is needed to characterize the neurons that are covered by PNNs in the ground squirrel brain, along with examining the individual components that make up these structures. Additionally, this work further highlights the PVN as an important component of hibernation regulation.

Funding This study was funded by a University of Wisconsin-La Crosse Faculty Research Grant to CS and a University of Wisconsin-La Crosse Undergraduate Research and Creativity Grant to AM.

Compliance with ethical standards

Conflict of interest The authors declare that they have no conflict of interest.

Ethical approval All applicable international, national, and/or institutional guidelines for the care and use of animals were followed. All procedures performed in studies involving animals were in accordance with the ethical standards of the University of Wisconsin-La Crosse Institutional Animal Care and Use Committee (protocol #14–15). This article does not contain any studies with human participants performed by any of the authors.

References

Arena ET, Rueden CT, Hiner MC, Wang S, Yuan M, Eliceiri KW (2017) Quantitating the cell: turning images into numbers with ImageJ. Wiley Interdiscip Rev Dev Biol 6:e260

Balmer TS, Carels VM, Frisch JL, Nick TA (2009) Modulation of perineuronal nets and parvalbumin with developmental song learning. J Neurosci 29:12878–12885

Bratincsak A, McMullen D, Miyake S, Toth ZE, Hallenbeck J, Palkovits M (2007) Spatial and temporal activation of brain regions in hibernation: *c-fos* expression during the hibernation bout in thirteen-lined ground squirrel. J Comp Neurol 505:443–458

Brückner G, Hausen D, Härtig W, Drlicek M, Arendt T, Brauer K (1999) Cortical areas abundant in extracellular matrix chondroitin sulphate proteoglycans are less affected by cytoskeletal changes in Alzheimer's disease. Neuroscience 92:791–805

Buijs R, Pévet P, Masson-Pévet M, Pool C, De Vries G, Canguilheim B, Vivien-Roels B (1986) Seasonal variation in vasopressin innervation in the brain of the European hamster (*Cricetus cricetus*). Brain Res 371:193–196

Cabungcal J-H, Steullet P, Morishita H, Kraftsik R, Cuenod M, Hensch TK, Do KQ (2013) Perineuronal nets protect fast-spiking interneurons against oxidative stress. Proc Natl Acad Sci USA 110:9130–9135

Carey HV, Andrews MT, Martin SL (2003) Mammalian hibernation: cellular and molecular responses to depressed metabolism and low temperature. Physiol Rev 83:1153–1181

Carulli D, Pizzorusso T, Kwok JC, Putignano E, Poli A, Forostyak S, Andrews MR, Deepa SS, Glant TT, Fawcett JW (2010) Animals lacking link protein have attenuated perineuronal nets and persistent plasticity. Brain 133:2331–2347

Cerri S, Bottiroli G, Bottone MG, Barni S, Bernocchi G (2009) Cell proliferation and death in the brain of active and hibernating frogs. J Anat 215:124–131

Cowley MA, Pronchuk N, Fan W, Dinulescu DM, Colmers WF, Cone RD (1999) Integration of NPY, AGRP, and melanocortin signals in the hypothalamic paraventricular nucleus: evidence of a cellular basis for the adipostat. Neuron 24:155–163

Dityatev A, Brückner G, Dityateva G, Grosche J, Kleene R, Schachner M (2007) Activity-dependent formation and functions of chondroitin sulfate-rich extracellular matrix of perineuronal nets. Dev Neurobiol 67:570–588

Frare C, Jenkins M, McClure K, Drew K (2019) Seasonal decrease in thermogenesis and increase in vasoconstriction explain seasonal response to 6 N-cyclohexyladenosine-induced hibernation in the Arctic Ground Squirrel (*Urocitellus parryii*). J Neurochem 151:316–335

Frerichs K, Kennedy C, Sokoloff L, Hallenbeck J (1994) Local cerebral blood flow during hibernation, a model of natural tolerance to "cerebral ischemia". J Cereb Blood Flow Metab 14:193–205

Geerling JC, Shin JW, Chimenti PC, Loewy AD (2010) Paraventricular hypothalamic nucleus: axonal projections to the brainstem. J Comp Neurol 518:1460–1499

Giamanco K, Morawski M, Matthews R (2010) Perineuronal net formation and structure in aggrecan knockout mice. Neuroscience 170:1314–1327

Heller HC (1979) Hibernation: neural aspects. Annu Rev Physiol 41:305–321

Hermes M, Kalsbeek A, Kirsch R, Buijs R, Pe P (1993) Induction of arousal in hibernating European hamsters (*Cricetus cricetus L.*) by vasopressin infusion in the lateral septum. Brain Res 631:313–316

Ishiwata T, Hasegawa H, Yazawa T, Otokawa M, Aihara Y (2002) Functional role of the preoptic area and anterior hypothalamus in thermoregulation in freely moving rats. Neurosci Lett 325:167–170

Jinka TR, Tøien Ø, Drew KL (2011) Season primes the brain in an arctic hibernator to facilitate entrance into torpor mediated by adenosine A1 receptors. J Neurosci 31:10752–10758

Joseph SA, Knigge KA, Kalejs LM, Hoffman R, Reid P (1966) A stereotaxic atlas of the brain of the 13-lined ground squirrel (*Citellus*

tridecemlineatus). Medical Research Laboratory, United States Edgewood Arsenal

Lensjø KK, Lepperød ME, Dick G, Hafting T, Fyhn M (2017) Removal of perineuronal nets unlocks juvenile plasticity through network mechanisms of decreased inhibition and increased gamma activity. J Neurosci 37:1269–1283

Lu J, Greco MA, Shiromani P, Saper CB (2000) Effect of lesions of the ventrolateral preoptic nucleus on NREM and REM sleep. J Neurosci 20:3830–3842

Magariños AM, McEwen BS, Saboureau M, Pevet P (2006) Rapid and reversible changes in intrahippocampal connectivity during the course of hibernation in European hamsters. Proc Natl Acad Sci USA 103:18775–18780

Matthews RT, Kelly GM, Zerillo CA, Gray G, Tiemeyer M, Hockfield S (2002) Aggrecan glycoforms contribute to the molecular heterogeneity of perineuronal nets. J Neurosci 22:7536–7547

Millesi E, Prossinger H, Dittami JP, Fieder M (2001) Hibernation effects on memory in European ground squirrels (*Spermophilus citellus*). J Biol Rhythm 16:264–271

Miyata S, Nishimura Y, Nakashima T (2007) Perineuronal nets protect against amyloid β-protein neurotoxicity in cultured cortical neurons. Brain Res 1150:200–206

Morawski M, Brückner G, Jäger C, Seeger G, Arendt T (2010) Neurons associated with aggrecan-based perineuronal nets are protected against tau pathology in subcortical regions in Alzheimer's disease. Neuroscience 169:1347–1363

Morawski M, Dityatev A, Hartlage-Rübsamen M, Blosa M, Holzer M, Flach K, Pavlica S, Dityateva G, Grosche J, Brückner G (2014) Tenascin-R promotes assembly of the extracellular matrix of perineuronal nets via clustering of aggrecan. Philos Trans R Soc Lond B Biol Sci 369:20140046

Paxinos G, Watson C (2005) The rat brain in stereotaxic coordinates. Elsevier Academic Press, London

Pizzorusso T, Medini P, Berardi N, Chierzi S, Fawcett JW, Maffei L (2002) Reactivation of ocular dominance plasticity in the adult visual cortex. Science 298:1248–1251

Popov V, Bocharova L, Bragin A (1992) Repeated changes of dendritic morphology in the hippocampus of ground squirrels in the course of hibernation. Neuroscience 48:45–51

Roozendaal B, McEwen BS, Chattarji S (2009) Stress, memory and the amygdala. Nat Rev Neurosci 10:423

Ruby NF (1995) Paraventricular nucleus ablation disrupts daily torpor in Siberian hamsters. Brain Res Bull 37:193–198

Ruediger J, Van der Zee E, Strijkstra A, Aschoff A, Daan S, Hut R (2007) Dynamics in the ultrastructure of asymmetric axospinous synapses in the frontal cortex of hibernating European ground squirrels (*Spermophilus citellus*). Synapse 61:343–352

Schwartz C, Hampton M, Andrews MT (2013) Seasonal and regional differences in gene expression in the brain of a hibernating mammal. PLoS One 8:e58427

Schwartz C, Hampton M, Andrews MT (2015) Hypothalamic gene expression underlying pre-hibernation satiety. Genes Brain Behav 14:310–318

Sorg BA, Berretta S, Blacktop JM, Fawcett JW, Kitagawa H, Kwok JC, Miquel M (2016) Casting a wide net: role of perineuronal nets in neural plasticity. J Neurosci 36:11459–11468

Tupone D, Madden CJ, Morrison SF (2013) Central activation of the A1 adenosine receptor (A1AR) induces a hypothermic, torpor-like state in the rat. J Neurosci 33:14512–14525

von der Ohe CG, Darian-Smith C, Garner C, Heller H (2006) Ubiquitous and temperature-dependent neural plasticity in hibernators. J Neurosci 26:10590–10598

von der Ohe CG, Garner CC, Darian-Smith C, Heller HC (2007) Synaptic protein dynamics in hibernation. J Neurosci 27:84–92

Wang D, Fawcett J (2012) The perineuronal net and the control of CNS plasticity. Cell Tissue Res 349:147–160